

# REQUIREMENTS FOR TRACKING RADAR FOR FALLING SPHERES

By John L. Hain and William E. Brockman

Booz, Allen Applied Research, Inc.

## SUMMARY

As a part of the system design of an upper air synoptic sounding system for NASA Langley Research Center, a technique was developed for expressing explicitly the effect of pertinent radar accuracy limits on the uncertainties in the meteorological data produced by the system. The results of this aspect of the study are briefly reviewed herein.

## INTRODUCTION

The passive falling sphere is the lightest and least expensive payload which has been shown to provide satisfactory data in the upper atmosphere, i.e., 30 to 100 km altitude. The payload and the means of lofting it have been well developed and their costs are well understood and manageable. The usable data, however, come from a high-cost ground tracker of limited availability. With few exceptions the data have been obtained using rather expensive trackers procured for and dedicated to significantly different purposes. The purpose of this paper is to explore the relation between the requirements for data on the motion of the sphere and selected sources of error in a radar tracker.

The discussion will consist of three parts, covering: first, the sphere trajectory; second, some pertinent radar accuracy limits; and third, the consequent limits on density and wind accuracies. Since only certain limiting conditions are considered, the results are essentially boundaries rather than explicit statements of accuracies applicable to specific configurations.

A detailed derivation of the equations used in developing these boundaries is included in reference 1.

## SYMBOLS

- B Receiver Bandwidth
- $C_D$  Drag Coefficient
- E Elevation Angle of Sphere from Tracker
- $F_o$  Receiver Noise Figure

$g$	Gravitational Constant
$G_t, G_r$	Gain of Transmitting and Receiving Antennas
$L$	Tracker System Losses
$N$	Number of Independent Data Points
$P_t$	Radiated Power of Tracker
$R$	Slant Range Between Sphere and Tracker
$\dot{R}$	Radial Velocity Between Sphere and Tracker
$S/N$	Effective Signal to Noise Ratio
$\Delta t$	Time Interval in Seconds
$x, z$	$x$ and $z$ Coordinates of Sphere Position
$W$	Wind Vector
$W_z$	Vertical Component of Wind
$\alpha, \beta$	Angles Defining Line of Sight Between Sphere and Tracker
$\Delta q$	Bias Error in Any Parameter $q$
$\theta$	Antenna Beamwidth
$\lambda$	Operating Wavelength of Tracker
$\rho$	Density
$\sigma$	Radar Cross Section of Sphere
$\sigma_q$	Standard Deviation of Any Parameter $q$
$\sigma_q^2$	Variance of Random Error in $q$

Dots over a symbol denote the degree of the derivative with respect to time.

### THE SPHERE TRAJECTORY

Assuming a rocket-lofted sphere, a skewed trajectory envelope such as that depicted in Figure 1 was used. Wind profiles of  $\pm 50\%$  and  $\pm 99\%$  were included to assure adequacy of spatial coverage. A collocated launcher and tracker were assumed to minimize personnel, logistic and real estate costs for a synoptic system. The initial conditions (at the top of the sphere trajectory) are as follows:

Altitude	140 km
Horizontal displacement	40 km
Horizontal velocity	200 meters/sec
Gravitational acceleration	-9.8 meters/sec
Area/Mass ratio	6.54
Radius of the earth	6,378,388 meters

The resultant theoretical descending trajectory, using the  $+50\%$  wind profile, is shown in Table 1. If such an actual trajectory can be observed as a suitable set of coordinates vs. time, both density and wind data may be determined.

The density of the atmosphere in the immediate vicinity of the falling sphere may be derived as a function of:

- Vertical velocity of the sphere
- Vertical acceleration of the sphere
- Drag coefficient of the sphere.

The local wind vector may be derived as a function of:

- Vertical and horizontal velocity of the sphere
- Vertical and horizontal acceleration of the sphere
- Gravitational constant.

Thus, if our trajectory is measured as a set of spatial coordinates vs. time, it is apparent that the falling sphere technique is as sensitive to errors in the first and second time derivatives of the coordinates as it is to errors in the coordinates themselves. For ease in exploring these relationships, a two-dimensional flight profile for the sphere was assumed. This is equivalent to aligning the launcher inclination and the effective plane of one of the tracker's angular sensors with the prevailing wind.

If the first and/or second derivatives are obtained by fitting a function to the data points and taking the derivative, the error can be separated into two parts. One part is

the error due to noise in the data, the other due to lack of fit by the function to the physical laws that produced the data points.

The error due to noise is a function of:

- Fitting length (number of points)
- Data frequency
- Noise in measured parameter
- Method used (polynomial and degree).

The error due to lack of fit is a function of:

- Fitting length (number of points)
- Data frequency
- Numerical characteristics of the function that produced the data points
- Method used (polynomial and degree).

Since the purpose of this discussion is to explore the impact of radar errors, only the error due to noise in the measurements will be pursued.

The expression for the error in density which has been derived (ref. 2) is

$$\left(\frac{\sigma_{\rho}}{\rho}\right)^2 = \left(\frac{2\sigma_{W_z}}{\dot{z} - W_z}\right)^2 + \left(\frac{2\sigma_{\dot{z}}}{\dot{z} - W_z}\right)^2 + \left(\frac{\sigma_{\ddot{z}}}{\ddot{z} - g}\right)^2 + \left(\frac{\Delta\ddot{z}}{\ddot{z} - g} - \frac{2\Delta\dot{z}}{\dot{z} - W_z} - \frac{\Delta C_D}{C_D}\right)$$

The bias error is the error due to lack of fit and will, as previously stated, not be considered. Uncertainty in the drag coefficient, probably one of the most significant problems relative to the falling sphere technique, is, fortunately, not germane to the tracking accuracy exploration. Eliminating these terms, the expression for error in density may be rewritten as

$$\left(\frac{\sigma_{\rho}}{\rho}\right)^2 = \frac{4}{(\dot{z} - W_z)^2} \sigma_{\dot{z}}^2 + \frac{1}{(\ddot{z} - g)^2} \sigma_{\ddot{z}}^2 + \frac{4}{(\dot{z} - W_z)^2} \sigma_{W_z}^2$$

Similarly, the variance in the horizontal wind is

$$\sigma_W^2 = \sigma_{\dot{x}}^2 + \left(\frac{\dot{z}}{\dot{z} - g}\right)^2 \sigma_{\dot{x}}^2 + \left(\frac{\ddot{x}}{\ddot{z} - g}\right)^2 \sigma_{\dot{z}}^2 + \left(\frac{\ddot{x}\dot{z}}{\ddot{z} - g^2}\right)^2 \sigma_{\ddot{z}}^2$$

where the expression for the horizontal wind is

$$W = \dot{x} - \frac{\ddot{x}\dot{z}}{\ddot{z} - g}$$

## PERTINENT RADAR ACCURACY LIMITS

The geometry of a generalized tracker operating on a passive falling sphere is shown in Figure 2. As shown, the definitions are those commonly used for a phased-array tracker. The two-dimensional analysis merely assumes that the wind lies along either the  $\alpha$  or  $\beta$  axes. The elevation angle is thus the complement of  $\alpha$  (or  $\beta$ ). In the case of the usual electromechanical tracker, the analysis assumes no change in azimuth, so that all angular data is again in the elevation angle. The other two measurements of which a radar tracker is capable, range and range rate (or radial velocity), have been shown (ref. 3) to be interrelated through pulse width so that the corresponding accuracy limits are not independent. The standard deviation of range varies directly with the pulse width while that of radial velocity varies inversely. Although not strictly true in the general case, for many applications either may be computed from the other with an accuracy comparable to that which could be obtained by direct measurement. Therefore, the radar measurements which were explored in detail were those of slant range and elevation angle.

The classical radar range equation may be written (ref. 4) in the form

$$\frac{S}{N} = \frac{P_t G_t G_r \lambda^2 \sigma}{R^4 B F_o L}$$

where  $P_t$  is in watts,  $\lambda$  is in centimeters,  $R$  is in nautical miles,  $\sigma$  is in meters<sup>2</sup>, and  $B$  is in hertz. The achievable accuracy is a function of the effective signal to noise ratio, and that varies inversely as the fourth power of the slant range. Thus, the quality of the meteorological data will degrade very rapidly with increasing distance to the falling sphere. Thermal noise, an inseparable part of every real signal, establishes a limit beyond which no hardware can extract usable data. The standard deviations for range and angle measurements on a single pulse basis (ref. 4) are

$$\sigma_R = \frac{137\tau}{\sqrt{S/N}}$$

$$\sigma_E = \frac{\theta}{2\sqrt{S/N}}$$

where  $\sigma_R$  is in meters,  $\sigma_E$  and  $\theta$  are in milliradians, and  $\tau$  is in microseconds.

Using these basic tools of sphere dynamics and of radar accuracy limits it was then possible to establish certain limits on the quality of meteorological observations.

The obvious trade-offs were those between maintaining vertical resolution and enhancing apparent accuracy by smoothing over a large number of data points. Thus, the length of the smoothing interval became a good indicator of relative merit.

### ESTIMATION OF ACCURACY LIMITS

One final simplification: Fully acceptable techniques for separating vertical winds from density variance have yet to be developed, and the radar does not offer a solution. Therefore, the vertical component of the wind vector, like the uncertainty in the drag coefficient, does not appear in the final error model. It simply is not a part of the radar error contribution.

Since the errors in velocities and accelerations are smaller when a quadratic polynomial is fitted to the data points than when successive linear polynomials are used, the quadratic fit was used throughout the study. Velocities were then evaluated from the first derivative and acceleration from the second derivative of this smooth curve.

The error in the first derivative as a function of the error in the parameter is given by

$$\sigma_{\dot{q}}^2 = \frac{12}{N(N+1)(N+2)\Delta t^2} \sigma_q^2$$

and the error in the second derivative is given by

$$\sigma_{\ddot{q}}^2 = \frac{720}{(N-1)N(N+1)(N+2)(N+3)\Delta t^4} \sigma_q^2$$

The error model consisted of expressions for the error in density and in horizontal winds as functions of the variance of range, range rate, range acceleration, elevation angle, elevation rate, and elevation acceleration, as well as values dependent on the trajectory and smoothing interval.

But since only the range and elevation angle were measured, with the rates and acceleration being derived mathematically, the model was modified by substituting the derived variances of  $\dot{R}$ ,  $\ddot{R}$ ,  $\dot{E}$ , and  $\ddot{E}$ . The model then took the form:

$$\left(\frac{\sigma_\rho}{\rho}\right)^2 = F_1 \sigma_R^2 + F_2 \sigma_E^2$$

$$\sigma_W^2 = G_1 \sigma_R^2 + G_2 \sigma_E^2$$

where the F's and G's are lengthy functions of the coordinates and of the fitting functions, but not of errors in determining the coordinates.

Since angular accuracy is the most cost-sensitive parameter of a tracker (aside from attaining a workable signal to noise ratio) the relationship of meteorological function error to angular error was explored.

The first method of analysis was to assume a slant range error of 5 meters and to compute the smoothing interval when the elevation angle error was 0.05 mil and the density error was 2%. The density error limit was then increased to 3% and various values of elevation angle error were tried until the resulting smoothing interval was approximately equal to the 0.05 mil, 2% result. The process was repeated for density errors of 4% and 5%. The corresponding wind error was computed at each altitude level, for each combination of elevation angle error and density error. The complete profiles are given in Figure 3.

The following combinations of density error and elevation error yield approximately equal smoothing intervals. The maximum horizontal wind error for each combination is as shown.

Elevation, $\sigma_E$ (mils)	Density, $\frac{\sigma_\rho}{\rho}$ (%)	Wind, $\sigma_W$ (meters/sec)
0.05	2	19
0.10	3	37
0.15	4	54
0.20	5	70

The second method was to allow the elevation angle error to assume successively larger values, the only other parameter which was allowed to change as a consequence was the smoothing interval. This has the net effect of increasing the uncertainty as to the altitude at which the computed density was valid and, thus, results in a net uncertainty as to the density profile. The data are shown in Figure 4.

### CONCLUSIONS

A method has been developed, programed, and tested for quickly determining the error contours applicable to a passive falling sphere, upper-air sounding system. It was then apparent that a synoptic system using the given trajectory placed stringent requirements on the tracker.

A stated design goal of a vertical resolution of 500 meters, with a standard deviation of 2% in density data and of 5 meters/second in wind velocity (below 70 km altitude) can be met, but it requires a sufficiently high signal to noise ratio in the tracker that the uncertainty due to thermal noise is no greater than 5 meters in range and 0.05 mil in angle.

Relaxation of vertical resolution permits longer smoothing intervals with consequent dramatic reduction in requisite angular accuracy.

#### REFERENCES

1. Booz, Allen Applied Research, Inc.: System for Upper Atmospheric Sounding (SUAS). Vol. II - Technical Report. NASA CR-66753-2, 1969.
2. Luers, J. K.: Estimation of Errors in Density and Temperature Measured by the High Altitude ROBIN Sphere. Proceedings of the Third National Conference on Aerospace Meteorology, Amer. Meteorol. Soc., 1968, pp. 472-477.
3. Skolnik, Merrill I.: Radar Systems. McGraw-Hill Book Co., Inc., 1962.
4. Barton, David K.: Radar System Analysis. Prentice-Hall, Inc., c.1964.



# TABLE 1

## TRAJECTORY

### Using +50% Wind Profile

ALTITUDE (METERS)	HORIZONTAL DISPLACEMENT (METERS)*	HORIZONTAL VELOCITY (METERS/SECOND)	HORIZONTAL ACCELERATION (METERS/SECOND <sup>2</sup> )	VERTICAL VELOCITY (METERS/SECOND)	VERTICAL ACCELERATION (METERS/SECOND <sup>2</sup> )	SPEED (METERS/SECOND)**
140,000	41,200	200	-.009	-56	-9.367	208
130,000	49,384	199	-.052	-439	-9.286	482
120,000	53,151	197	-.165	-613	-8.920	644
110,000	56,076	191	-.776	-734	-6.485	759
100,000	58,445	167	-3.415	-756	5.918	774
90,000	60,493	82	-5.575	-472	22.554	479
80,000	61,686	11	.055	-112	1.457	112
70,000	63,065	25	.163	-93	.656	93
60,000	68,279	41	.075	-49	.147	49
50,000	82,110	48	-.036	-26	.042	26
40,000	104,673	34	-.017	-13	.012	13

\*FROM A VERTICAL AXIS THROUGH LAUNCH SITE

\*\*WITH RESPECT TO SURFACE OF EARTH

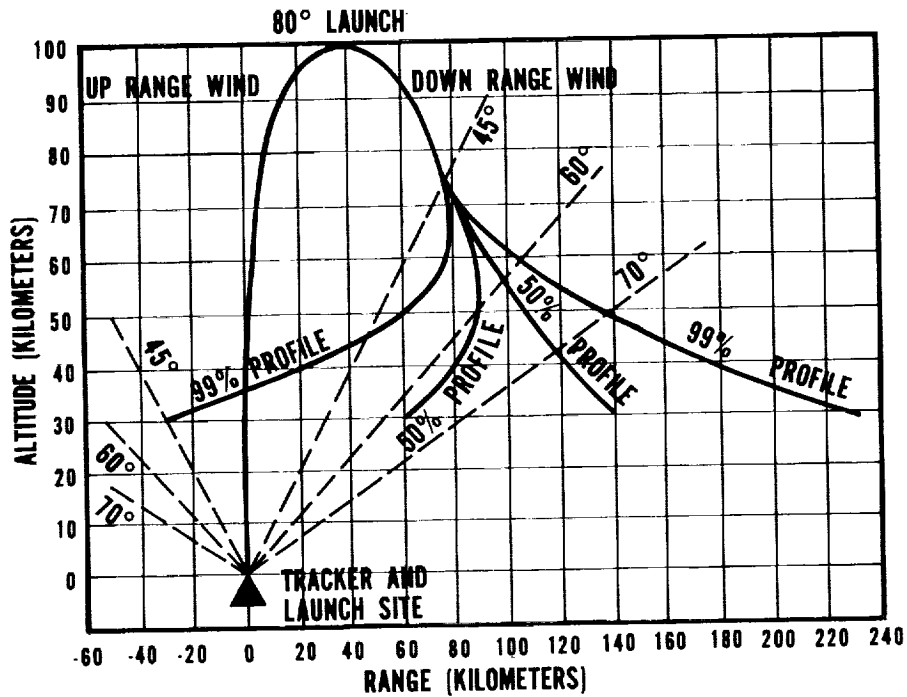


Figure 1.- Flight profile for inclined launch.

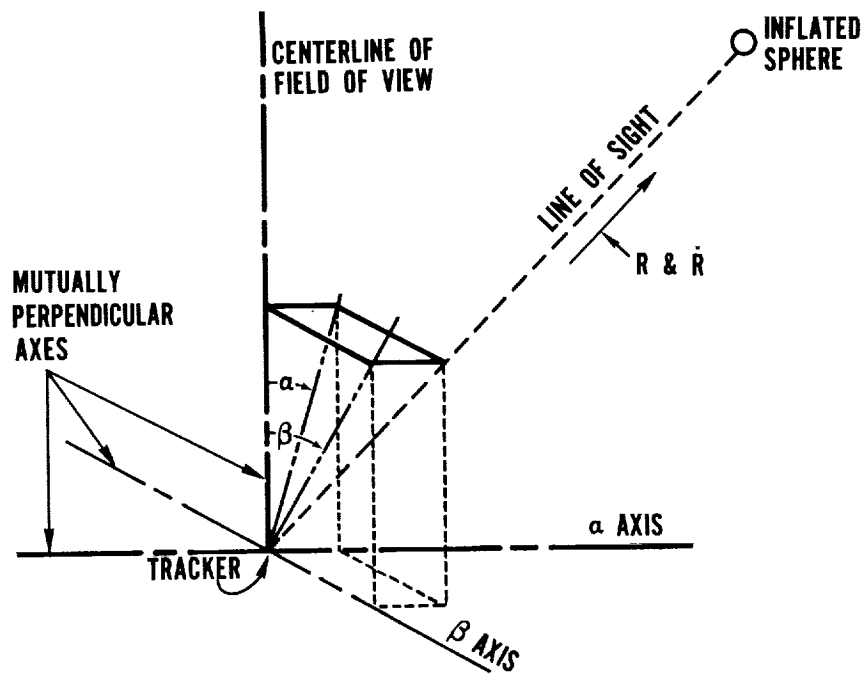


Figure 2.- Geometry of measured quantities.

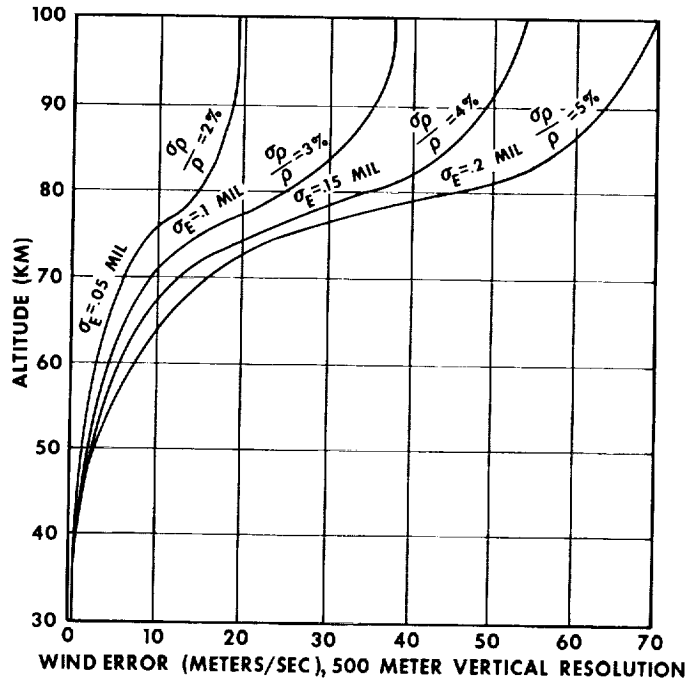


Figure 3.- Wind errors corresponding to various density errors.

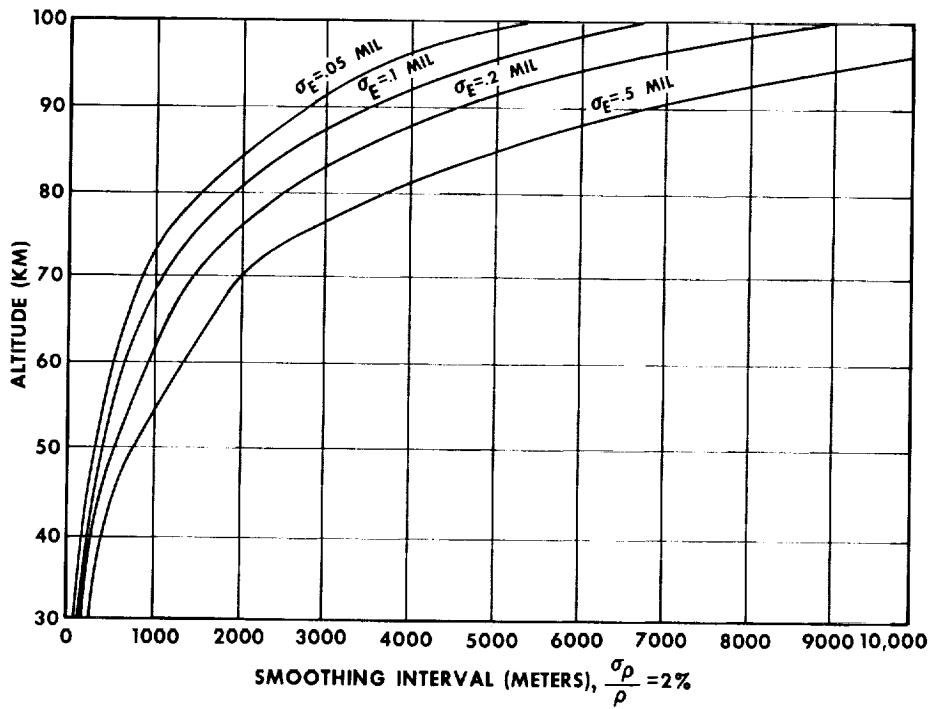


Figure 4.- Requisite smoothing intervals for apparent 2% density error.

